

Effect of Palladium Loading on Catalytic Properties of Pd/GCE for the Electro-oxidation of Methanol, Formic Acid, and Ethylene Glycol

Islam M. Al-Akraa^{1,*}, Yaser M. Asal¹, Sohair A. Darwish¹, Rafik M. Fikry¹, Reem H. Mahmoud¹, Mohamed Hassan¹, Ahmad M. Mohammad^{2,*}

¹ Department of Chemical Engineering, Faculty of Engineering, The British University in Egypt, Cairo 11837, Egypt

² Chemistry Department, Faculty of Science, Cairo University, Cairo 12613, Egypt

*E-mails: islam.ahmed@bue.edu.eg, ammohammad@cu.edu.eg

Received: 19 December 2021 / Accepted: 3 February 2022 / Published: 4 March 2022

This study investigates the influence of the catalyst (Palladium, Pd) mass that loaded onto a glassy carbon electrode (GCE) on the catalytic activity of methanol (MEO), formic acid (FAEO), and ethylene glycol (EGEO) electro-oxidation, the corresponding principal anodic reactions in the direct methanol (DMFCs), formic acid (DFAFCs), and ethylene glycol (DEGFCs) fuel cells, respectively. By increasing the Pd loading at 0.1 V, the Pd surface area increased from 0.55 cm² (2 min Pd deposition) to 1.94 cm² (25 min Pd deposition) which increased the peak currents (I_P) of MEO (from 0.181 to 0.608 mA), FAEO (from 0.236 to 1.303 mA), and EGEO (from 0.699 to 2.082 mA). Additionally, the increase in Pd loading shifted the oxidation peak potentials (E_P) to higher values (from -0.014 to 0.2 V for MEO, from -0.15 to 0.36 V for FAEO, and from 0.11 to 0.44 V for EGEO). It is thought that increasing I_P is related to the increased Pd surface area while the slow diffusion of ions (compared with the fast charge transfer) and/or increasing the distance for the electron transport over the electrode due to catalyst stacking were behind the potential shifts.

Keywords: Fuel cells; Electrocatalysis; Methanol electro-oxidation; Formic acid electro-oxidation; Ethylene glycol electro-oxidation.

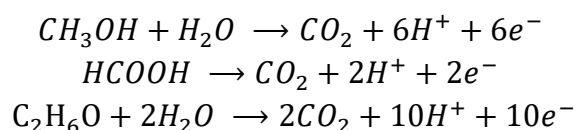
1. INTRODUCTION

The world is seeking and achieving renewability. The previous statement is not an exaggeration. In fact, many governments around the globe are actively adopting and enforcing new regulations and legislations [1] that ensure our natural resources are preserved for the future generations, or in other words, are sustainable [2]. In order to achieve sustainability, resources should be used in a limited rate so as not to result in its depletion over time, alongside considering the environment in every aspect [3].

For a very long time, the major source of energy and power generation has been the combustion of fossil fuels [4]. However, knowing that it results in heavily contaminating products and billions of tons of carbon emissions every year, the use of fossil fuels is evident to be harmful to the environment. Additionally, the tremendous global demand for power production needed by our modern societies cannot be met with the traditional sources of energy [5]. In fact, the current natural gas and oil reserves are estimated to last optimistically for only about fifty years [6]. Accordingly, the use of fossil fuels as the major source of energy is not only non-sustainable, but also non-reliable [7]. This has urged the exploration of new safe, green, and sustainable energy sources that are capable of supplying the power needed for our daily life and industrial demands [8-11].

One of the attempts to save energy in completely renewable plants was feeding any excessive energy into water electrolyzers that produce hydrogen and oxygen. Then, when energy is needed, those products are fed to a typical H₂/O₂ fuel cell generating electricity and producing water again as the only by-product [12, 13]. This simple cycle has been the seed idea that activated researching fuel cells (FCs), however, now they are more utilised in powering portable systems such as electric vehicles and backup stations [14]. The working principal of FCs is the galvanic conversion of chemical energy into electricity. The key difference between FCs and other regular galvanic batteries is the continuous supply of the reactants, which in this case are the fuel and oxygen [15]. What makes FCs of great interest is its direct power supply, which is particularly useful for portable applications [16, 17]. Another very useful aspect is the ability of distributing several power-generation stations, thus eliminating the energy losses associated with transmitting electricity over long lines [18]. Additionally, FCs show enhanced efficiency both considering electrical energy conversion efficiency (up to 60%) and electricity and heat efficiency (up to 80%). FCs are greener as they produce 90% less pollutants compared to fossil fuel combustion [14, 19]. FCs are also reliable, robust, safe, quiet, easy to install, and have extended lifetime [20] all of which made FCs a very promising alternative for power production, particularly for transportation as well as portable electronic applications [21].

The famous H₂/O₂ fuel cells or hydrogen-based fuel cells (HFCs) employ hydrogen as the fuel. The intensive research on HFCs was encouraged by the fact that hydrogen is the lightest green (carbon-free) fuel [22]. Interestingly, electric vehicles and other important applications in portable electronics probably would not have been made possible without the development of FCs. However, the commercialization was restricted by difficulties and hazards associated with producing, using, distributing, and storing H₂ gas. Aside of that, the electro-oxidation of H₂ produces only two electrons, thus hydrogen is considered to have a relatively low gas-phase energy density. All of these limitations have encouraged researchers to consider replacing hydrogen with other small hydrogen-containing liquid fuels with low carbon-content, in what is known as liquid fuel cells (LFCs) such as direct methanol (DMFCs), direct FA (DFAFCs), and direct EG (DEGFCs) fuel cells [23-30]. The following equations represent the perfect anodic MEO, FAEO, and EGEO [31].



Here, we study the influence of increasing Pd mass loading by electrodeposition over the GCE on the catalytic activity of MEO, FAEO, and EGEO.

2. EXPERIMENTAL

2.1. Electrodes and reagents

GCE (d = 5 mm) electrode was served as the working electrode after conventional cleaning procedures [32]. The cleaning process involved a mechanically polishing for the electrode with no. 2000 emery paper, followed by aqueous slurries of successively finer alumina powder (down to 0.06 μm) with a polishing micro-cloth. Next, the polished electrode was thoroughly rinsed with distilled water. A spiral Pt wire and an Ag/AgCl/NaCl (3M) were used as the counter and reference electrodes, respectively. Highly purified palladium (II) acetate (trimer, Pd 45.9 - 48.4%), sulphuric acid (98.0 %), methanol (CH_3OH , 99.0%), FA (HCOOH , 98%), EG ($\text{C}_2\text{H}_6\text{O}_2$, 99%), were purchased from Alfa Aesar and Sigma Aldrich.

2.2. Electrodeposition of Pd

The Pd was electrodeposited onto the GCE in 0.1 M H_2SO_4 containing 1.0 mM $\text{Pd}(\text{CH}_3\text{COO})_2$ solution at a constant potential electrolysis at 0.1 V. In order to evaluate the influence of catalyst loading, different catalysts were prepared by varying the electrodeposition durations. The electrodes abbreviated as Pd-2m, Pd-5m, Pd-10m, Pd-15m, Pd-20m, and Pd-25m corresponded to the electrodeposition of Pd onto the GCE for 2, 5, 10, 15, 20, and 25 min, respectively.

2.3. Electrochemical measurement

The electrochemical measurements were carried out in a traditional three-electrode glass cell at room temperature (around 25 $^\circ\text{C}$) using a Bio-Logic SAS potentiostat (model SP-150) operated with EC-Lab software. The electrocatalytic activity of each prepared catalyst towards MEO, FAEO, and EGEO was examined in 0.1 M NaOH solution containing 0.3 M methanol, FA, and EG, respectively, at a scan rate of 100 mV s^{-1} . Current densities were calculated based on the working electrode's real surface area, which was calculated from the corresponding cyclic voltammograms (CVs) in 0.5 M H_2SO_4 using a reference charge of 420 $\mu\text{C cm}^{-2}$ [33].

3. RESULTS AND DISCUSSION

3.1. Electrochemical characterization

The surface of the prepared Pd catalyst was characterised using the electrochemical method. Figure 1 shows the typical CVs measured in 0.5 M H_2SO_4 for all prepared catalysts. All catalysts showed

the characteristic features of Pd at which the surface oxidation (Pd/PdO) extending over a wide range of potentials (0.6 to 1.2 V) was coupled with its subsequent reduction (PdO/Pd) between ca. 0.2 - 0.5 V. This associated with hydrogen adsorption/desorption ($H_{\text{ads/des}}$) peaks in the potential range from -0.2 to 0.0 V.

As clearly observed by the increase of the Pd mass loading, a concurrent increase in the currents of Pd oxidation, PdO reduction, and $H_{\text{ads/des}}$ was observed. The accompanied increase in the Pd surface area (A_{pd} , reflected from the charge associated with the PdO reduction peak and tabulated in Table 1) was behind such trend. A deeper look revealed the PdO reduction potential cathodic shift with the increase of loading. This might relate to changing the catalyst surface composition.

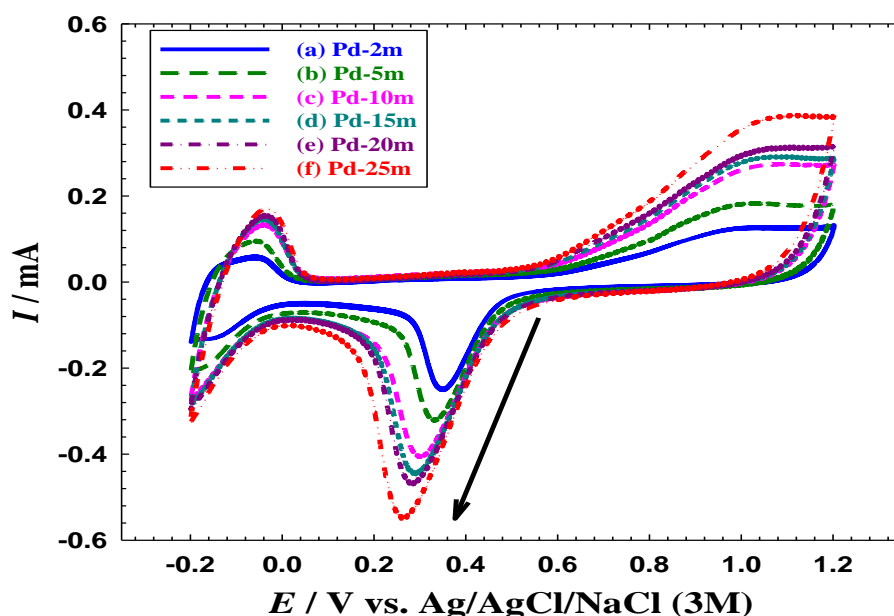


Figure 1. CVs measured in 0.5 M H_2SO_4 at (a) Pd-2m, (b) Pd-5m, (c) Pd-10m, (d) Pd-15m, (e) Pd-20m, and (f) Pd-25m catalysts. (Scan rate = 100 mV s^{-1}).

Table 1. Calculated A_{pd} for each catalyst (data extracted from Fig. 1).

Catalyst	$A_{\text{pd}} (\text{cm}^2)$
Pd-2m	0.552
Pd-5m	0.761
Pd-10m	1.242
Pd-15m	1.423
Pd-20m	1.554
Pd-25m	1.941

3.2. Methanol, Formic acid, and Ethylene glycol Electro-oxidation

The electrocatalytic activity of each prepared catalyst towards MEO was examined by measuring the linear sweep voltammograms (LSVs) at a potential scan rate of 100 mV s^{-1} in 0.1 M NaOH solution containing 0.3 M methanol ($\text{pH} = 3.5$).

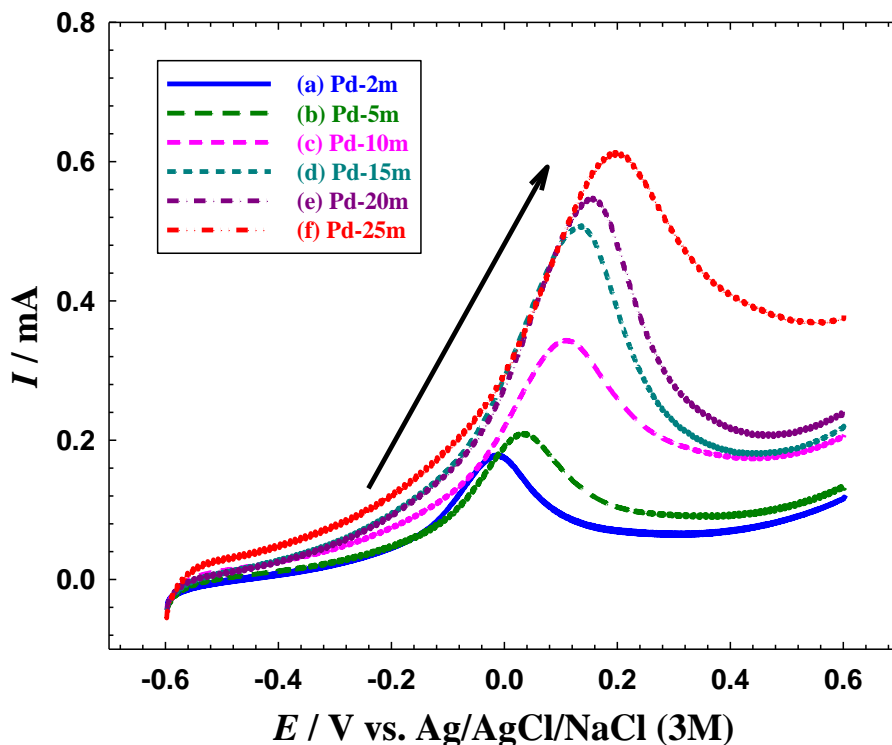


Figure 2. LSVs obtained at (a) Pd-2m, (b) Pd-5m, (c) Pd-10m, (d) Pd-15m, (e) Pd-20m, and (f) Pd-25m catalysts in 0.1 M NaOH solution containing 0.3 M Methanol ($\text{pH} = 3.5$). (Scan rate = 100 mV s^{-1}).

Figure 2 shows the LSVs of the entire catalyst set. At the Pd-2m catalyst, the MEO occurred at ca. -0.014 V with ca. 0.181 mA current. By increasing the Pd mass loading, the peak potential (E_p) shifted to more anodic potentials and the peak current (I_p) acquired a higher value reaching ca. 0.2 V and 0.608 mA at the Pd-25m catalyst. Table 2 summarizes the I_p and E_p values for all prepared catalysts.

Similarly, the electrocatalytic activity towards FAEO was examined by measuring the LSVs of each electrode in 0.1 M NaOH solution containing 0.3 M FA ($\text{pH} = 3.5$) at a potential scan rate of 100 mV s^{-1} . The obtained LSVs are shown in Fig. 3. At the Pd-2m catalyst, the FAEO occurred at E_p ca. -0.15 V with ca. I_p of 0.236 mA . By increasing the Pd mass loading, the E_p shifted to more anodic potentials and the I_p acquired a higher value reaching ca. 0.36 V and 1.303 mA at the Pd-25m catalyst. Table 3 summarizes the I_p and E_p values for all prepared catalysts.

Table 2. Electrochemical indices for each catalyst during MEO (data extracted from Fig. 2).

Catalyst	I_p (mA)	E_p (V)
Pd-2m	0.181	-0.014
Pd-5m	0.211	0.034
Pd-10m	0.350	0.110
Pd-15m	0.509	0.141
Pd-20m	0.546	0.163
Pd-25m	0.608	0.201

Lastly, the electrocatalytic activity towards EGEO was examined by measuring the LSVs of each electrode in 0.1 M NaOH solution containing 0.3 M EG (pH = 3.5) at a potential scan rate of 100 mV s⁻¹. The obtained LSVs are shown in Fig. 4. At the Pd-2m catalyst, the EGEO occurred at ca. E_p of ca. 0.11 V with I_p of ca. 0.699 mA. By increasing the Pd mass loading, the E_p shifted to more anodic potentials and the I_p acquired a higher value reaching ca. 0.44 V and 2.082 mA at the Pd-25m catalyst. Table 4 summarizes the I_p and E_p values for all prepared catalysts.

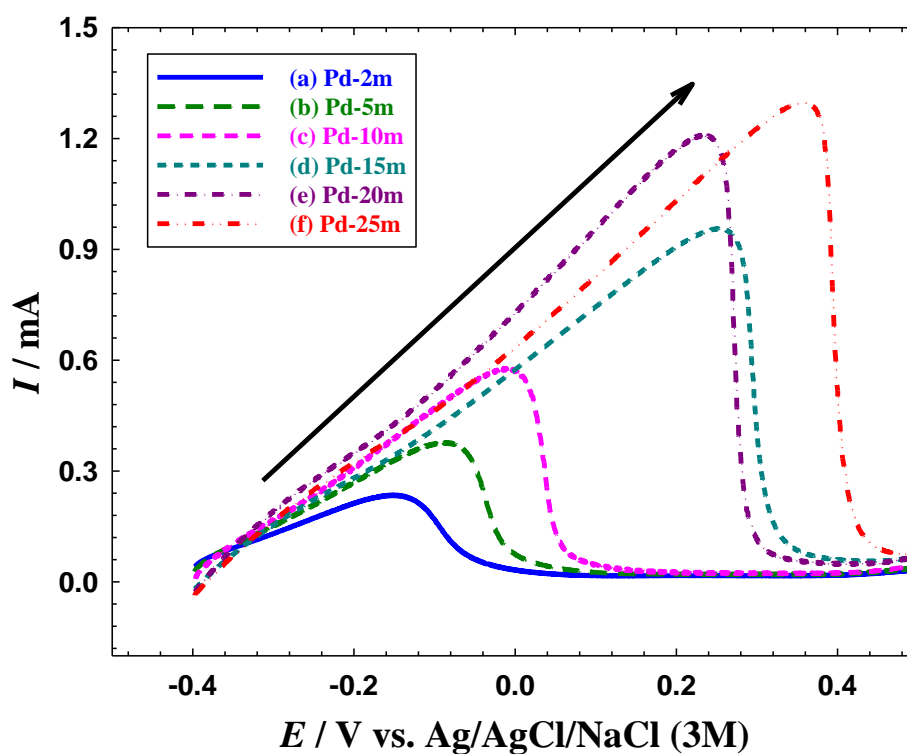
**Figure 3.** LSVs obtained at (a) Pd-2m, (b) Pd-5m, (c) Pd-10m, (d) Pd-15m, (e) Pd-20m, and (f) Pd-25m electrodes in 0.1 M NaOH solution containing 0.3 M FA (pH = 3.5). (Scan rate = 100 mV s⁻¹).

Table 3. Electrochemical indices for each catalyst during FAEO (data extracted from Fig. 3)

Catalyst	I_P (mA)	E_P (V)
Pd-2m	0.236	-0.152
Pd-5m	0.378	-0.087
Pd-10m	0.584	-0.011
Pd-15m	0.963	0.253
Pd-20m	1.218	0.232
Pd-25m	1.303	0.364

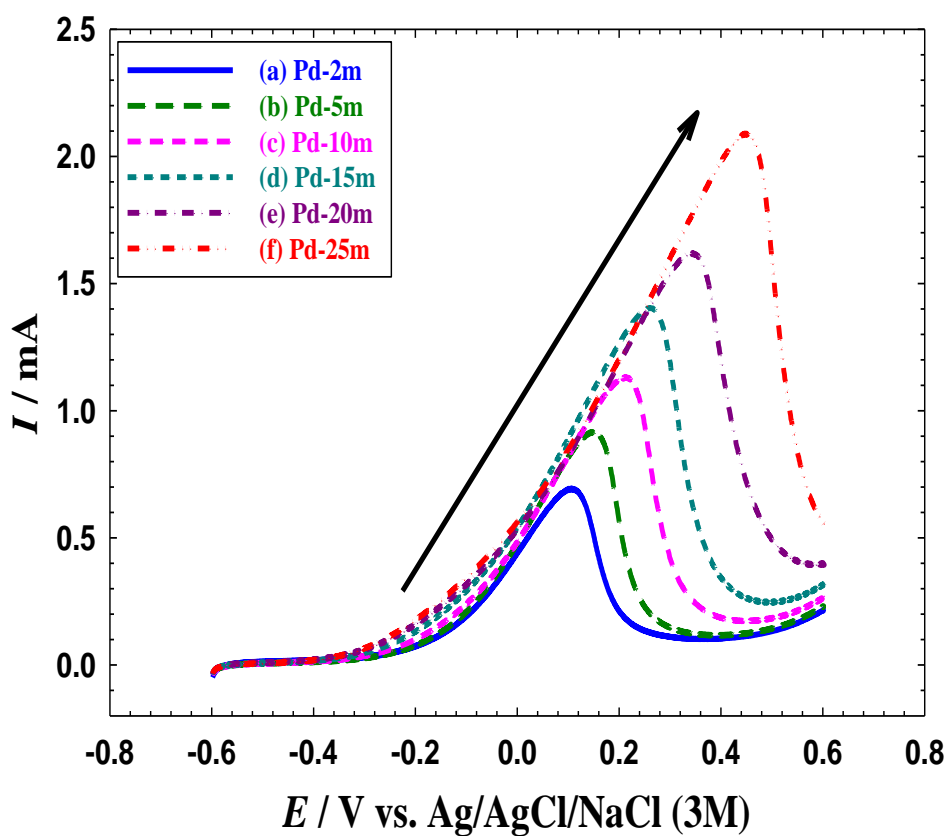
**Figure 4.** LSVs obtained at (a) Pd-2m, (b) Pd-5m, (c) Pd-10m, (d) Pd-15m, (e) Pd-20m, and (f) Pd-25m electrodes in 0.1 M NaOH solution containing 0.3 M EG (pH = 3.5). (Scan rate = 100 mV s⁻¹).

Table 4. Electrochemical indices for each catalyst during EGEO (data extracted from Fig. 4).

Catalyst	I_p (mA)	E_p (V)
Pd-2m	0.699	0.112
Pd-5m	0.914	0.163
Pd-10m	1.129	0.220
Pd-15m	1.396	0.264
Pd-20m	1.621	0.341
Pd-25m	2.082	0.442

From Figs. 2- 4 and from Tables 2-4 we can say that increasing the Pd mass loading affected both the I_p and E_p values for all prepared catalysts during MEO, FAEO, and EGEO. It was thought that increasing the A_{pd} was behind increasing the I_p while at the same time the slow diffusion of ions (compared with the fast charge transfer) and/or increasing the distance for the electron transport over the electrode due to catalyst stacking were behind the potential shifts [40]. Table 5 shows a comparison of the electrocatalytic activity of the Pd-25m catalyst and several others reported in literature.

Table 5. A comparison of the electrocatalytic activities of several catalysts toward MOR, EGEO, and FAEO.

Catalyst	Activity ($I_p / \text{mA cm}^{-2}$)			
	Methanol	FA	EG	Ref.
Pd	0.30	-	-	[34]
Pd@PDPA	0.139	-	-	[35]
PtPd/HPC500	-	0.169	-	[36]
Pd-Ag/C	-	0.80	-	[37]
Pd/C	-	-	0.60	[38]
Pt90Pd10/C	-	-	0.65	[39]
Pd-25m	0.313	0.672	1.073	This work

4. CONCLUSION

Several catalysts were prepared by loading different amounts of Pd; aiming to study the variations of their catalytic performance toward MO, FAEO, and EGEO. Increasing the Pd mass loading affected both the I_p (which increased as a result of the A_{pd} increase) and E_p (which shifted to more anodic values because of the slow diffusion of ions (compared with the fast charge transfer) and/or increasing

the distance for the electron transport over the electrode due to catalyst stacking) for all prepared catalysts during MEO, FAEO, and EGEO.

References

1. EPA, in *EPA (United States Environmental Protection Agency)*.
2. E.A. Olivetti, J.M. Cullen, *Science*, 360 (2018) 1396.
3. UN, Sustainability, United Nations. <https://www.un.org/en/academic-impact/sustainability>.
4. T.M. Letcher, in *Managing Global Warming: An Interface of Technology and Human Issues*, T. Letcher, Ed. (Academic Press, 2018) 3.
5. S. Nishimura, N. Ikeda, K. Ebitani, *Catal. Today*, 232 (2014) 89.
6. T. Covert, M. Greenstone, C.R. Knittel, <http://home.uchicago.edu>.
7. D.-H. Lee, C.-P. Hung, *Int. J. Hydrog. Energy*, 37 (2012) 15753.
8. I.M. Al-Akraa, Y.M. Asal, A.M. Arafa, *Int. J. Electrochem. Sci.*, 13 (2018) 8775.
9. I.M. Al-Akraa, Y.M. Asal, S.D. Khamis, *Int. J. Electrochem. Sci.*, 13 (2018) 9712.
10. I.M. Al-Akraa, T. Ohsaka, A.M. Mohammad, *Arab. J. Chem.*, 12 (2019) 897.
11. A.H. Ali, Y.M. Asal, I.M. Al-Akraa, *ARPN J. Eng. Appl. Sci.*, 16 (2021) 1630.
12. J.A. Turner, *Science*, 305 (2004) 972.
13. I.M. Sadiq, A.M. Mohammad, M.E. El-Shakre, M.S. El-Deab, B.E. El-Anadouli, *J Solid State Electrochem.*, 17 (2013) 871.
14. S. Curtin, J. Gangi, Fuel cell technologies market report 2014, *US Department of Energy, 2014*.
15. J. Lindorfer, D.C. Rosenfeld, H. Böhm, in *Future Energy: Improved, Sustainable and Clean Options for our Planet*, T. M. Letcher, Ed. (Elsevier, 2020) 495.
16. H. Zhang, X. Li, X. Liu, J. Yan, *Appl. Energy*, 241 (2019) 483.
17. Y.M. Asal, A.M. Mohammad, S.S.A.E. Rehim, I.M. Al-Akraa, *J. Saudi Chem. Soc.*, In press (2022).
18. A.M. Mohammad, I.M. Al-Akraa, M.S. El-Deab, *Int. J. Hydrog. Energy*, 43 (2018) 139.
19. D. Papageorgopoulos, An Introduction to the 2010 Fuel Cell, *US Department of Energy: Energy, Lakewood, Colorado, 2010*.
20. M. Bron, C. Roth, *New and Future Developments in Catalysis*. S. Suib, Ed., (Elsevier, Amsterdam, 2013).
21. B. Braunschweig, D. Hibbitts, M. Neurock, A. Wieckowski, *Catal. Today*, 202 (2013) 197.
22. A.M. Abdullah, A.M. Mohammad, T. Okajima, F. Kitamura, T. Ohsaka, *J. Power Sources*, 190 (2009) 264.
23. C. Zhai, M. Zhu, F. Pang, D. Bin, C. Lu, M.C. Goh, P. Yang, Y. Du, *ACS Appl. Mater. Interfaces*, 8 (2016) 5972.
24. I.M. Al-Akraa, Y.M. Asal, S.A. Darwish, *Int. J. Electrochem. Sci.*, 14 (2019) 8267.
25. I.M. Al-Akraa, Y.M. Asal, A.A. Khalifa, *Int. J. Electrochem. Sci.*, 14 (2019) 8276.
26. I.M. Al-Akraa, A.M. Mohammad, *Arab. J. Chem.*, 13 (2020) 4703.
27. I.M. Al-Akraa, A.E. Salama, Y.M. Asal, A.M. Mohammad, *Arab. J. Chem.*, 14 (2021) 103383.
28. B.A. Al-Qodami, H.H. Alalawy, I.M. Al-Akraa, S.Y. Sayed, N.K. Allam, A.M. Mohammad, *Int. J. Hydrog. Energy*, 47 (2022) 264.
29. Y.M. Asal, I.M. Al-Akraa, A.M. Mohammad, M.S. El-Deab, *J Taiwan Inst Chem Eng.*, 96 (2019) 169-175.
30. Y.M. Asal, A.M. Mohammad, S.S.A. El Rehim, I.M. Al-Akraa, *Int. J. Electrochem. Sci.*, 16 (2021) Article Number: 211133.
31. I.M. Al-Akraa, Y.M. Asal, A.M. Mohammad, *J. Nanomater.*, (2019) 2784708.
32. E. Kjeang, R. Michel, D.A. Harrington, D. Sinton, N. Djilali, *Electrochim. Acta*, 54 (2008) 698.
33. T. Binningerz, E. Fabbri, R. Kötz, T.J. Schmidt, *J. Electrochem. Soc.*, 16 (2014) H121.

34. R.B. Araujo, D. Martín-Yerga, E.C.d. Santos, A. Cornell, L.G.M. Pettersson, *Electrochim. Acta*, 360 (2020) 136954.
35. S.L. Madaswamy, M. Alfakeer, A.A.A. Bahajjaj, M. Ouladsmame, S.M. Wabaidur, C.-x. Chen, R. Dhanusuraman, *Synth. Met.*, 281 (2021) 116925.
36. A.S. Shatla, K.M. Hassan, A.A. Abd-El-Latif, A.A. Hathoot, H. Baltruschat, M. Abdel-Azzem, J. *Electroanal. Chem.*, 833 (2019) 231.
37. S. Hu, F. Che, B. Khorasani, M. Jeon, C.W. Yoon, J.-S. McEwen, L. Scudiero, S. Ha, *Appl. Catal. B: Environ.*, 254 (2019) 685.
38. J. Maya-Cornejo, N. Arjona, M. Guerra-Balcazar, L. Alvarez Contreras, J. Ledesma-García, L.G. Arriaga, *Procedia Chem.*, 12 (2014).
39. V.L. Marinho, E. Antolini, M.J. Giz, G.A. Camara, L.A. Pocrifka, R.R. Passos, *J. Electroanal. Chem.*, 880 (2021) 114859.
40. L. Yu, S. Sun, H. Lia, Z.J. Xu, *Fundam.res.*, 1 (2021) 448

© 2022 The Authors. Published by ESG (www.electrochemsci.org). This article is an open access article distributed under the terms and conditions of the Creative Commons Attribution license (<http://creativecommons.org/licenses/by/4.0/>).